

# Effect of silver nanoparticles ink on Cerium Titanium Oxide thin films

Cliff Orori Mosiori

*Department of Mathematics and Physics, Technical University of Mombasa, P. O. Box 90420 – 80100 Mombasa, Kenya*

Correspondence email: [corori@tum.ac.ke](mailto:corori@tum.ac.ke)

## ABSTRACT

Wide band gap technology has its challenges. However, such materials include  $\text{CeTiO}_2$  are known to have a wide band gap of about 3.55 eV. Effort is now directed towards  $\text{CeTiO}_2$  thin-films by incorporating nanoparticles. Finding wide band gap materials that are both transparent to visible light and electrically conductive for today's popular devices has now grown it investigating silver nanoparticles ( $\text{Ag NPs}$ ) for potential tuning of band gap. In this work, silver nanoparticles were used to dope  $\text{CeTiO}_2$ . To generate  $\text{Ce}_x\text{Ag}_{0.02x}\text{TiO}_2$ , pure cerium oxide, silver metal and titanium dioxide composites were used and it was observed that its thin films possess higher absorption coefficients with a tunable optical band gap varying between 3.42 - 3.78 eV suitable for wide band gap optical applications.

**Keywords:**  $\text{CeTiO}_2$ , Composite,  $\text{Ce}_x\text{Ag}_{0.02x}\text{TiO}_2$  thin films, laser radiation

## 1. INTRODUCTION

Silver nanoparticles have shown potential for various effective applications in technology. Take a case where dispersed  $\text{Ag NPs}$  on  $\text{TiO}_2$  thin films alone. It has found to enhance the photocurrent generation with five folds as compared to  $\text{TiO}_2$  under UV light irradiation [2]; it modifies many nano-composites materials under visible light irradiation for complete inhibition of microorganism activities [7]. By including silver nanoparticles in a gas sensor [13], it has been found to modify in their physical, chemical and structural properties while advantageously increasing gas sensor activity under visible-light irradiation. It has enhances sensitivity and selectivity electrochromic devices [7]. They have been proposed as effective component of modify composites of  $\text{TiO}_2$  since its applications include modifying nanostructures through different processing methods like sol-gel procedures [10]. In this study, pulsed laser deposition technique was used to deposit silver nanoparticles  $\text{CeTiO}_2$  thin films.

## 2. METHODOLOGY

The procedure that follows was done in university laboratory in China.

## **2.1 Cleaning of Substrates**

The SiO<sub>2</sub> quartz substrates were cleaned with acetone in a ultrasonic bath. The target was thoroughly cleaned before any preliminary trials were done and also after the trials.

## **2.2 Preparation of Vacuum Chamber**

Prior to each irradiation the vacuum chamber was evacuated down to a residual pressure of 10<sup>-4</sup> Pa. This pressure was maintained constant during the thin films synthesis process. High purity oxygen (99.9%) was then circulated inside the irradiation chamber through a calibrated gas inlet.

## **2.3 Reagents and Chemicals**

The chemicals and reagents included cerium, titanium, silver, silicon substrate, high purity oxygen (99.9%) among other laboratory chemicals and apparatus.

## **2.4. Growth procedures**

Growth of silver doped CeTiO<sub>2</sub> thin films was inside a stainless steel reaction chamber with a pulsed frequency laser fixed at  $\lambda = 255$  nm,  $\tau_{WHM} \sim 8$  ns,  $\nu = 20$  Hz; laser fluency fixed at 5 J/cm<sup>2</sup> at 0.1 MPa pressure. The concentration of silver nano-particle was varied between 1.5 to 3 wt.% range and sintered at 1000 °C for 2 hours. The substrates were positioned at a separation distance 30 mm from the target surface and parallel to it. The substrate temperature was fixed at about 630 °C during the film growth and only 10,000 laser pulses were applied to each thin film. The films were cooled down with a ramp of about 10 °C per minute at 0.5 MPa that used during the deposition experiments.

## **2.5 Thin film characterization**

The optical measurements were performed with a double beam Perkin Elmer Lambda 19 spectrophotometer in the wavelength range of 300nm to 1100 nm while compositional and crystallinity status were investigated by XRD and EXRD measurements by configuring the X-ray diffraction in  $\theta$ -2 $\theta$  configuration with a Philips MRD diffractometer (CuK $\alpha$ ,  $\lambda=1.5418$  Å radiation).

## 3.0 RESULTS

### 3.1 Elemental Composition of CeTiO<sub>2</sub>

The obtained SAED pattern resulted into inter-planar distances of 0.385 and 0.192 nm assigned to the (001) and (002) lattice plane reflections of the orthorhombic CeTiO<sub>2</sub> phase [4,7], with lattice parameters  $a = 7.318 \text{ \AA}$ ,  $b = 7.451 \text{ \AA}$ , and  $c = 3.684 \text{ \AA}$ , as referred in the JC-PDS 20-1324. Hence, there was no indication of the presence of silver or silver oxide observed.

### 3.2 Structural Properties of CeTiO<sub>2</sub> Thin films

The crystalline structure of the thin films was investigated using the XRD technology. The observed diffractogram curves composed of diffraction lines at 23.1°, 47.2° and 50.4° attributed to the (001), (002) and (112) lattice plane reflections. This implied an orthorhombic phase with a preferred orientation along the [001] crystal direction. With increase in Ag concentration, the intensity of the 23.1° line corresponding to (001) lattice plane reflection decreased gradually with full width at half maximum increasing [9].

#### 3.2.1 Structural Properties Ag- CeTiO<sub>2</sub> Thin films

Adding silver nano-particles to the film, the XRD peaks were modified. It was attributed the line 23.6° that appeared at (020) lattice plane reflection. About 0.2° degree shift towards higher values on the line was observed that corresponded to (001) lattice plane reflection. This was also attributed to the slight change of the d-spacing lattice parallel to the surface of substrate. It was concluded that silver nanoparticles as a dopant lead to an increase in the average dimensions crystals. The average size of nanocrystallites in the films was determined by the Scherrer equation [10]:

$$D_{hkl} = \frac{0.9\lambda}{\beta_{hkl} \cos \theta_{hkl}} \quad (1.1)$$

where  $\lambda$  is the X-ray wavelength,  $\theta_{hkl}$  is the Bragg diffraction angle and  $\beta_{hkl}$  is the full width at half-maximum.

### 3.3. Optical properties

#### 3.3.1 Chromaticity coordinates and tristimulus

It is known that chromaticity coordinates are used to specify the colour observed according to the CIE chromaticity diagram. Equally, standard tristimulus value is used as a measure of the brightness of a surface or colour. By using Python 2.7 program [1, 2, 9], optical transmittance

spectra, chromaticity coordinates and standard tristimulus value were calculated and tabulated as shown in table I. The dark blue colour was attributed to oxygen deficiency in the thin films. This further implied that CeTiO<sub>2</sub> underwent partial decomposition at the target as it was being irradiated by the subsequent laser pulses.

**Table I: Chromaticity coordinates and tristimulus**

<b>Ag conc. wt.%]</b>	<b>Tristimulus Y</b>	<b>Chromaticity coordinates (x, y)</b>
3.0	817	(0.35, 0.34)
2.5	321	(0.29, 0.32)
2.0	19	(0.23, 0.16)
1.5	9	(0.18, 0.16)
1.0	3	(0.14, 0.13)
0.5	1	(0.12, 0.11)
0.0	1	(0.11, 0.1)

### 3.3.2 Optical Transmittance

The average transmittance of the un-doped CeTiO<sub>2</sub> film was close to 90 % in the visible spectral range while the one containing silver (Ag) had an average decrease of greater than 20 %. This was attributed to the introduction of Ag nanoparticles into CeTiO<sub>2</sub> crystals.

### 3.3.3 Determination of thickness

Using surface profilometry data, the average thickness of the un-doped and doped thin films was evaluated to be around 98 nm.

### 3.3.4 Optical Band Gap, E<sub>g</sub>

Fundamentally absorption coefficient follows the relation in Eq. 4 where m = 2 for the indirect transitions and ½ for directly allowed transitions [9];

$$\alpha h\nu \sim (h\nu - E_g)^m \quad (3)$$

The Scout Software was used determine the possible transitions by simulating  $(\alpha h\nu)^{1/m}$  against  $h\nu$ , photon energy for m = 2 and for m = ½. Table II shows the obtained band gaps.

**Table II: Band gaps**

<b>E<sub>g</sub> [eV]</b>	<b>E<sub>g</sub> [eV]</b>
---------------------------	---------------------------

<b>CeTiO<sub>2</sub></b>	<b>Ce<sub>x</sub>Ag<sub>0.02x</sub>TiO<sub>2</sub></b>
2.66	3.42
2.78	3.55
2.87	3.76
3.03	3.79

This was similar to determining the band gap from plots of Eq. 4 for direct band gap values can be estimated [10];

$$(\alpha h\nu)^2 \sim h\nu - E_g \quad (4)$$

Band structure calculations were done on CeTiO<sub>2</sub> thin films (*reported elsewhere*- Mosiori *et al.*, 2016) revealed oxygen deficiency. The narrow changes observed in band gaps was attributed to charge carrier transfer from Ag to CeTiO<sub>2</sub> layer that might have resulted into a downward shift of the conduction band and at the same time, an upward shift of the valence band hence increasing the band gap,  $E_g$ .

### 3.3.5 Urbach energy, $E_0$

As observed in Mosiori *et al.* 2016, at photon energy  $h\nu$ , below the absorption edge, it is possible to evaluate the Urbach energy. This is because the structural disorders observed generate band tails with localised states and therefore the Urbach energy,  $E_0$ , can easily be estimated from [5];

$$\alpha(h\nu) = \alpha_o e^{\left(\frac{h\nu}{E_0}\right)} \quad (1.3)$$

This means that the dependence of Urbach energy on Ag concentration may introduce some lattice disorder in the composite material.

**Table III: Average size and Urbach Energy**

Ag concentration [wt.%]	Nano-crystallites size [nm]	Urbach energy [meV]	Tristimulus Y
3.0	85	297	817
2.5	63	361	321
2.0	51	398	19
1.5	41	421	9
1.0	33	441	3

0.5	29	496	1
0.0	17	573	1

If this expression is used to plot a curve, then the inverse of the slope will be a linear fit to the logarithmic plot of the absorption coefficient [7]. The value of Urbach energy calculated in this work as shown in table III and further illustrated by figure 1 was fairly similar for CeTiO<sub>2</sub> thin films as reported in literature elsewhere by other growth methods [3, 6, 8,11].

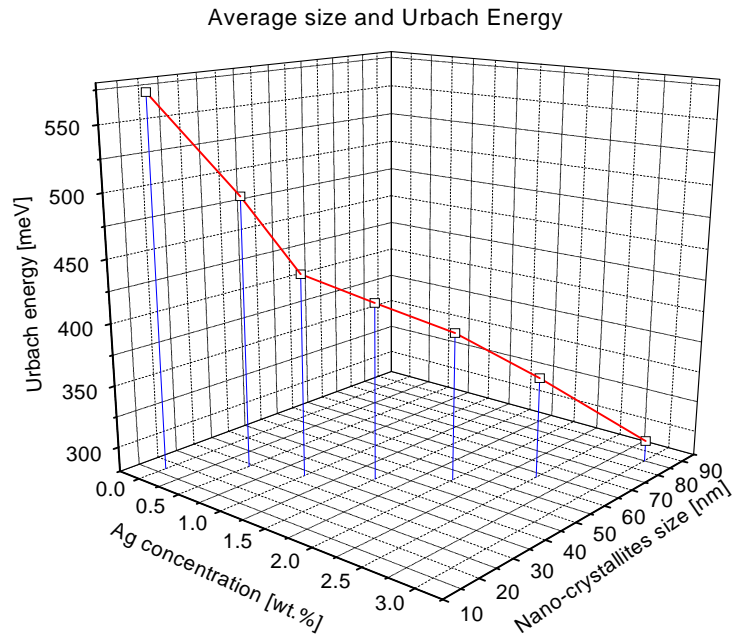


Figure 1: Relationship between average Silver particle and Urbach energy

### 3.4 Electrical properties

#### 3.4.1 Current-Voltage curve by CSAFM on CeTiO<sub>2</sub> thin films

CSAFM technique was used to determine the local conductivity of CeTiO<sub>2</sub> thin films using biased Pt-Ir coated silicon tips in contact mode. All the curves were non-ohmic as depicted by table IV. It was observed that the turn-on voltage value ranged between 0.1V to 0.3V while their corresponding resistance at 0 V range from about 0.4 - 2.5 GΩ. The small element of conduction was attributed to the semiconducting properties [12] of CeTiO<sub>2</sub> thin films.

#### 3.4.1 Current-Voltage curve by CSAFM on Ag doped CeTiO<sub>2</sub> thin films

Looking at figure 2, it can be noticed that almost similar I-V curves were obtained for Ag - CeTiO<sub>2</sub> thin films but the curves were slightly or nearly-Ohmic in character. The slight

deviation from the linearity was attributed to the contribution of the semiconducting behaviour [11] of  $\text{CeTiO}_2$  while the Ohmic behaviour was attributed to the presence of evenly dispersion Ag nanoparticles present. From figure 1, the gradual transition behaviour of I-V curve is a property that can be used in sensor applications to ensure better selectivity and sensitivity.

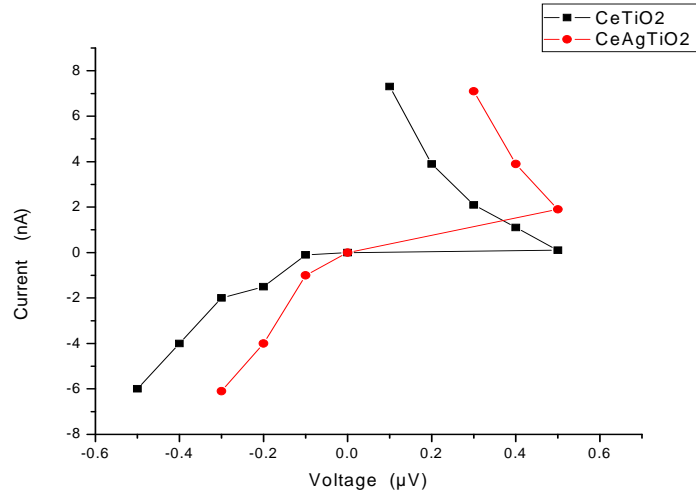


Figure 2: Comparison of I-V curve by CSAFM technique

## Conclusions

A nano-composite films of  $\text{Ce}_x\text{Ag}_{0.02x}\text{TiO}_2$  were grown by pulsed laser deposition. The effect of Ag concentration on crystalline status and optical properties was investigated. It was observed that there was a gradual band gap increase. This was attributed to the thin film's change in chemical composition as Ag was introduced. Electrical properties portrayed promising features for the design of new composite materials for applications electrochromic devices and gas sensors. Therefore, silver nanoparticles were observed to modified thin films and hence its non-spherical geometries can be used functionalize different materials for different applications.

## Acknowledgements

*The author is grateful to the university laboratory in China that allowed deposition, characterization of the thin films using their facilities. The author is also grateful to the Department of Mathematics and Physics of Technical University of Mombasa for the moral support during the time of developing this report.*

## References

1. Arabatzis, I. M., et al. "Silver-modified titanium dioxide thin films for efficient photodegradation of methyl orange." *Applied Catalysis B: Environmental* 42.2 (2003): 187-201.
2. Argall, F. "Switching phenomena in titanium oxide thin films." *Solid-State Electronics* 11.5 (1968): 535-541.
3. Bhuiyan, M. S., M. Paranthaman, and K. Salama. "Solution-derived textured oxide thin films—a review." *Superconductor Science and Technology* 19.2 (2006): R1.
4. Hass, Georg. "Preparation, properties and optical applications of thin films of titanium dioxide." *Vacuum* 2.4 (1952): 331-345.
5. Justicia, Isaac, et al. "Designed self-doped titanium oxide thin films for efficient visible-light photocatalysis." *Advanced Materials* 14.19 (2002): 1399-1402.
6. Keomany, D., C. Poinsignon, and D. Deroo. "Sol gel preparation of mixed cerium—titanium oxide thin films." *Solar Energy Materials and Solar Cells* 33.4 (1994): 429-441.
7. Machida, Mitsuyoshi, Keiichiro Norimoto, and Tamon Kimura. "Antibacterial activity of photocatalytic titanium dioxide thin films with photodeposited silver on the surface of sanitary ware." *Journal of the American Ceramic society* 88.1 (2005): 95-100.
8. Ritala, Mikko, et al. "Growth of titanium dioxide thin films by atomic layer epitaxy." *Thin Solid Films* 225.1-2 (1993): 288-295.
9. Sberveglieri, G., et al. "Titanium dioxide thin films prepared for alcohol microsensor applications." *Sensors and Actuators B: Chemical* 66.1-3 (2000): 139-141.
10. Suzuki, Toshio, et al. "Electrical conductivity and lattice defects in nanocrystalline cerium oxide thin films." *Journal of the American Ceramic Society* 84.9 (2001): 2007-2014.
11. Yoshimoto, Mamoru, et al. "Room-temperature epitaxial growth of CeO<sub>2</sub> thin films on Si (111) substrates for fabrication of sharp oxide/silicon interface." *Japanese journal of applied physics* 34.6A (1995): L688.
12. Younis, Adnan, Dewei Chu, and Sean Li. "Oxygen level: the dominant of resistive switching characteristics in cerium oxide thin films." *Journal of Physics D: Applied Physics* 45.35 (2012): 355101.